Dynamic Characterization of a DNA Repair Enzyme: NMR Studies of [*methyl*-^{13}C]Methionine-Labeled DNA Polymerase β

Bidisha Bose-Basu, Eugene F. DeRose, Thomas W. Kirby, Geoffrey A. Mueller, William A. Beard, Samuel H. Wilson, and Robert E. London*

Laboratory of Structural Biology, NIEHS, NIH, Research Triangle Park, North Carolina 27709

Received February 18, 2004; Revised Manuscript Received May 7, 2004

ABSTRACT: Crystallographic characterization of DNA polymerase β (pol β) has suggested that multiple-domain and subdomain motions occur during substrate binding and catalysis. NMR studies of [*methyl*-^{13}C]methionine-labeled pol β were conducted to characterize the structural and dynamic response to ligand binding. The enzyme contains seven methionine residues, one of which is at the amino terminus and is partially removed by the expression system. Three of the methyl resonances were readily assigned using site-directed mutants. Assignment of the resonances of Met155, Met158, and Met191 was more difficult due to the spatial proximity of these residues, so that assignments were based on NOESY−HSQC data and on the response to paramagnetic Co^{2+} addition, as well as shift perturbations observed for the site-directed mutants. The response of the methyl resonances to substrate binding was evaluated by the serial addition of a template oligonucleotide, a downstream 5′-phosphorylated oligonucleotide, and a primer oligonucleotide to create a two-nucleotide-gapped DNA substrate. Addition of the single-stranded template DNA resulted in selective broadening of the methyl resonance of Met18 in the 8 kDa lyase domain, and this resonance then shifted and sharpened upon addition of a 5′-phosphate-terminated downstream complementary oligonucleotide. Conversion of the two-nucleotide-gapped DNA substrate to a single-nucleotide-gapped substrate by incorporation of ddCMP produced a small perturbation of the Met236 resonance, which makes contact with the primer strand in the crystal structure. The addition of a second equivalent of ddCTP to form the pol β−DNA−ddCTP ternary complex resulted in significant shifts for the resonances corresponding to Met155, Met191, Met236, and Met282. The Met155 methyl resonance is severely broadened, while the Met191 and Met282 resonances exhibit significant but less extreme broadening. Since only Met236 makes contact with the substrate, the effects on Met155, Met236, and Met282 result from indirect conformational and dynamic perturbations. Previous crystallographic characterization of this abortive complex indicated that a polymerase subdomain or segment (α-helix N) repositions itself to form one face of the binding pocket for the nascent base pair. Met282 serves as a probe for motion in this segment. Addition of Mg^{2+}−dATP to pol β in the absence of DNA produced qualitatively similar but much smaller effects on Met191 and Met155, but did not strongly perturb Met282, leading to the conclusion that Mg^{2+}−dATP alone is insufficient to produce the large conformational changes that are observed in the abortive complex involving the gapped DNA with a blocked primer and ddNTP. Thus, the NMR data indicate that the nucleotide−DNA interaction appears to be essential for conformational activation.

DNA polymerase β (pol β)[1] is a polymerase in vertebrate cells involved in the repair of nuclear DNA (*1*, *2*). Because of its small size, excellent expression properties, and lack of a proofreading exonuclease, pol β is considered a model enzyme for mechanistic studies of the nucleotidyl transferase reaction, DNA synthesis fidelity, and protein−DNA interactions involved in repair. Pol β typically inserts a deoxynucleoside monophosphate into a single-nucleotide-gapped DNA repair intermediate formed during base excision repair. The 39 kDa enzyme is composed of two domains: a 31 kDa polymerase domain and an amino-terminal 8 kDa lyase domain that excises the 5′-deoxyribose phosphate (5′-dRP) intermediate produced during repair. The polymerase domain is composed of three functionally distinguishable subdomains. The polymerase catalytic subdomain coordinates two divalent metal cations that assist the nucleotidyl transferase reaction. Two additional subdomains that have primary roles in duplex DNA binding and nascent base pair (nucleoside 5′-triphosphate and templating nucleotide) binding border the catalytic subdomain. These subdomains are referred to as the C (catalytic), D (duplex DNA binding), and N (nascent base pair binding) subdomains to highlight their intrinsic functions. These subdomains would correspond to the palm, thumb, and fingers subdomains, respectively, according to the nomenclature that utilizes the architectural analogy to a right hand (*3*).

Crystallographic comparisons of the structure of pol β in various liganded states have indicated that numerous conformational changes occur upon substrate binding. These

* To whom correspondence should be addressed. Phone: (919) 541-4879. Fax: (919) 541-5707. E-mail: london@niehs.nih.gov.

[1] Abbreviations: pol β, DNA polymerase β; dNTP, deoxynucleotide triphosphate; ddNTP, dideoxynucleotide triphosphate; NMR, nuclear magnetic resonance; HSQC, heteronuclear single-quantum coherence.

10.1021/bi049641n
Published on Web 06/25/2004

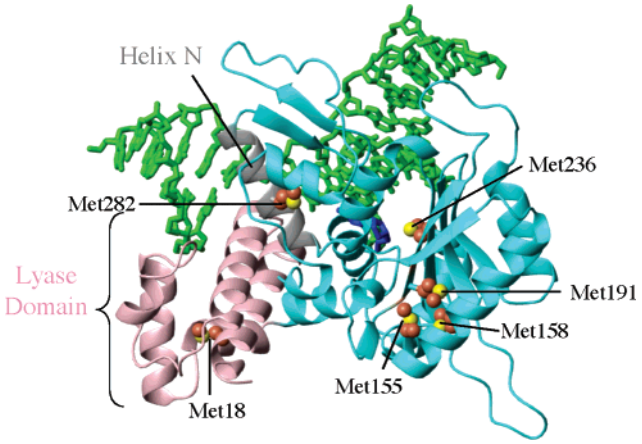

FIGURE 1: Structure of a DNA−pol β complex showing the six methionine residues (Met1 is not included). The polymerase domain is shown in cyan, with helix N in gray and the 8 kDa N-terminal lyase domain in pink. A gapped DNA is shown in green, with the primer 3′-nucleotide in blue. The figure was generated using MOLMOL (*45*).

transitions include (1) repositioning of the amino-terminal 8 kDa lyase domain toward the 31 kDa polymerase domain upon gapped DNA binding and (2) repositioning of α-helix N on the N-subdomain adjacent to the nascent base pair upon binding a complementary dNTP to form a ternary complex (*4*, *5*). The latter change results in the conversion from an "open" (lacking dNTP) to a "closed" (with dNTP bound) structure, forming an active site that coordinates two Mg^{2+} ions. In the complex with a single-nucleotide-gapped DNA ±dNTP), the template strand is bent by ∼90° at the active site. This bend permits polymerase residues of α-helix N to interact with the nascent base pair in the closed conformation (+dNTP). Mutagenesis data indicate that such contacts are crucial for achieving high DNA synthesis efficiency and fidelity (*6*−*11*). In addition to domain/subdomain movements, critical protein side chain and nucleotide repositioning occurs during substrate binding. For example, crystallographic structures of open and closed forms of many DNA polymerases suggest that the templating (i.e., coding) base is "out-of-position" in the open form, but moves to a coding position upon binding a correct dNTP (*1*).

It is still uncertain how the static conformational states revealed by the structural snapshots provided by crystallographic analysis contribute to the kinetic properties of the enzyme. For this reason, we have prepared [*methyl*-^{13}C]-methionine-labeled pol β to investigate the structural and dynamic properties of the enzyme in the local environments of the six methionine residues (seven if the amino-terminal Met1 residue is included). The methionine residues are distributed throughout the enzyme, including one residue in the amino-terminal lyase domain (Met18), one residue near the active site that is in contact with the primer strand (Met236), three residues in the C-subdomain that form a hydrophobic core near the enzyme active site (Met155, Met158, and Met191), and, finally, Met282 located on α-helix N, which undergoes a major conformational change in response to nucleotide binding (Figure 1). Methionine labeling is an attractive strategy for the study of large proteins due to the presence of three magnetically equivalent protons and internal diffusion of the methyl group resulting in sharper resonances (*12*−*15*). As demonstrated here, the methionine residues provide sensitive probes for the conformational and dynamic response of pol β to a broad range of ligands and substrates.

EXPERIMENTAL PROCEDURES

Materials. Oligonucleotides were obtained from Oligos, Etc. or from Integrated DNA Technologies, Inc. Deoxynucleoside triphosphates were from QIAGEN. Unlabeled amino acids, MOPS, tricine, adenine, guanine, cytosine, thymine, uracil, and ssDNA cellulose were from Sigma-Aldrich. [ϵ-^{13}C]Methionine was from Cambridge Isotope Laboratories. Isopropyl thio-β-D-galactoside (IPTG) was from Invitrogen. Q-Sepharose and Sephacryl-100 were from Amersham Pharmacia Biotech AB.

Expression of Rat DNA Polymerase-β. The cDNA of rat pol β described previously (*16*) was subcloned by Expand PCR (Roche), followed by restriction digestion with *Nde*I and *Sac*I, and ligation into pET30a(+) (Novagen) which had also undergone digestion with *Nde*I and *Sac*I. The N-terminal and C-terminal primers used for the amplification were 5′-CGCGCG*CATATG*AGCAAACGCAAGGCGCC-3′ and 5′-GGCCGC*GAGCTC*ATTCACTCCTGTCCTTGGGC-3′, which contain *Nde*I and *Sac*I restriction sites (italic), respectively. The plasmid so constructed was used to transform *E. coli* strains BL21(DE3) and B834(DE3) for expression (Novagen strains). B834(DE3) cells are methionine auxotrophs used for [ϵ-^{13}C]methionine-enriched labeling.

Cells containing plasmid were grown to mid-log phase ($A_{600} \approx 0.6$) at 37 °C in a defined medium enriched with [ϵ-^{13}C]methionine, containing 50 mg/mL kanamycin, to label the methionine residues of the protein. The defined medium (*17*) contained all amino acids except L-methionine, which is substituted by [ϵ-^{13}C]methionine, to repress endogenous synthesis by bacteria. Protein expression was induced by addition of IPTG to 1 mM, and the growth was continued for 3−4 h. The cells were harvested by centrifugation and stored at −20 °C.

Mutagenesis. Mutating each of the six methionine residues to valine was carried out by a PCR-based in vitro mutagenesis procedure using the QuikChange XL site-directed mutagenesis kit (Stratagene). The synthetic mutagenic ∼31−35-mer oligonucleotides used for M18V, M155V, M158V, M191V, M236V, and M282V mutations had the ATG codons for the methionines changed to GTG (Val). The presence of the desired mutations in the plasmids was confirmed by DNA sequence analysis using the Big Dye sequencing kit (Applied Biosystems).

Purification. The harvested cells were resuspended in lysis buffer (buffer 1) containing 50 mM Tris−HCl (pH 7.5), 10 mM sodium bisulfite, 1 mM EDTA, 1 mM DTT, 500 mM NaCl, 1 mM AEBSF, 1 mM benzamidine, 1 μg/mL pepstatin A, and 1 μg/mL leupeptin. The cell suspension was treated in a Branson sonicator, model 200, using a microtip probe at an output level of 6 for 10 × 30 s, with 30 s of cooling for each cycle to effect cell disruption. The lysate was centrifuged at 150000*g* for 30 min. The supernatant fraction was diluted with buffer (buffer 1 without NaCl) to give a final NaCl concentration of 75 mM, and the mixture was pumped onto a Q-Sepharose column (2.6 × 35 cm) which was connected in series to a single-strand DNA−cellulose column (1.6 × 13 cm) that had been equilibrated with buffer 2: 50 mM Tris−HCl, pH 7.5, 10 mM sodium bisulfite, 1

Table 1: Methionine Relaxation Table

residue	T_1 (s) 14.1 T	T_1 (s) 18.8 T	NOE 14.1 T	NOE 18.8 T	T_2 (ms) 14.1 T	S^2 model LS-3[b]	S^2 contact model[c]
Met1	1.58 ± 0.14	2.18 ± 0.12	1.79 ± 0.16	*a*	311 ± 30		
Met18	1.89 ± 0.17	2.37 ± 0.19	1.46 ± 0.03	1.71 ± 0.04	54 ± 13	0.50	0.260
Met155	4.01 ± 0.83	4.31 ± 0.95	1.44 ± 0.03	1.38 ± 0.03	44 ± 6	0.22	0.286
Met158	2.70 ± 0.26	2.77 ± 0.32	2.07 ± 0.02	1.71 ± 0.02	53 ± 8	0.42	0.297
Met191	3.01 ± 0.30	3.53 ± 0.12	1.65 ± 0.02	1.41 ± 0.02	40 ± 7	0.33	0.295
Met236	2.08 ± 0.12	2.23 ± 0.12	1.60 ± 0.02	1.47 ± 0.02	57 ± 15	0.48	0.169
Met282	1.93 ± 0.12	2.29 ± 0.37	1.57 ± 0.06	1.43 ± 0.06	57 ± 12	0.43	0.291

[a] The NOE data for Met1 at 201.1 MHz did not provide a sufficient signal/noise ratio for a determination. [b] Order parameters fit using the effective correlation time model LS-3 as described by Choy and Kay (*31*). [c] Order parameters determined using the contact model of Ming and Bruschweiler (*32*) based on a high-resolution crystal structure of pol β (based on coordinates of a 1.65 Å unpublished structure of pol β kindly provided by Joseph Krahn and co-workers).

mM EDTA, 1 mM DTT, 75 mM NaCl, 1 mM AEBSF, 1 mM benzamidine, 1 μg/mL pepstatin A, and 1 μg/mL leupeptin. The columns were washed with one column volume of buffer 2, and then the DNA−cellulose column was disconnected from the Q-Sepharose column and eluted with a gradient of 75−1000 mM NaCl. Fractions containing the polymerase were pooled and concentrated to 6 mL with Centriprep YM-10 (Amicon), and then the polymerase was chromatographed on a 2.6 × 63 cm column of Sephacryl S-100 which was preequilibrated with buffer 2. Fractions containing pure protein were pooled and concentrated using a Centricon YM-10 filter unit. At this stage, the proteins were greater than 95% homogeneous on the basis of the Coomassie Blue-stained SDS−PAGE gel.

Sample Preparation. After purification, the protein was concentrated and NMR samples were prepared. The final NMR sample contained 0.3−0.6 mM pol β in 40 mM Tris-d_{11}, pH 7.6, 130 mM KCl, 1 mM DTT, 0.1 mM AEBSF, 0.04% NaN_3, and 50 μM DSS, as an internal chemical shift standard in D_2O.

NMR Spectroscopy. NMR experiments were performed at 25 °C on a Varian UNITY INOVA 600 MHz NMR spectrometer, using a 5 mm Varian (600 MHz) $^1H\{^{13}C,^{15}N\}$ triple-resonance probe, equipped with actively shielded *Z*-gradients. The $^1H-^{13}C$ HSQC spectra were acquired using Varian's gChsqc sequence (*18*). The data were acquired as a 230 (t_1) × 512 (t_2) complex matrix, with acquisition times of 63.9 ms (t_1) and 64.0 (t_2) ms, 128 scans per increment, and a 1.0 s delay between scans. The 3D ^{13}C-edited NOESY spectrum was acquired with Varian's gnoesyChsqc experiment (*19*). The spectrum was acquired as a 128 (t_1) × 36 (t_2) × 512 (t_3) complex matrix, using a mixing time of 100 ms, with acquisition times of 16.0 ms (t_1), 10.0 ms (t_2), and 64.0 ms (t_3), eight scans per increment, and a 1.0 s recovery delay between scans. All 2D and 3D spectra were processed using NMRPipe version 2.1 (*20*) and analyzed using NMRView version 5.0.4 (*21*). All spectra were processed using squared cosine bell apodization functions in all dimensions and forward−backward linear prediction in the indirect ^{13}C dimension (*22*).

Relaxation experiments were performed at 600 and 800 MHz according to Farrow et al. (*23*) and Yamazaki et al. (*24*). For [ϵ-^{13}C]methionine, there is no significant $^{13}C-^{13}C$ coupling, so pulses intended to eliminate the effects of this coupling were set to a power level of zero. Data for T_1 delays were acquired out to 5 s due to the long relaxation times observed. Data for T_2 delays were acquired out to 100 ms. The $^1H\{^{13}C\}$ NOE presaturation time was 3 s, with a 2 s interscan delay. Without presaturation the interscan delay was 5 s. The $^1H\{^{13}C\}$ NOE experiment has relatively poor sensitivity in general, but we were able to acquire data with 48 scans per acquisition, close to 24 h of signal averaging, for each experiment, i.e., with and without presaturation. Relaxation data for the apoenzyme state were acquired at 600 and 800 MHz. The data were processed with NMRPipe (*20*) and relaxation times analyzed with NMRView (*21*).

RESULTS

Assignment of [methyl-^{13}C]Methionine-Labeled Pol β. The $^1H-^{13}C$ HSQC spectra of [*methyl*-^{13}C]methionine-labeled pol β obtained initially were characterized by six relatively intense resonances as well as a number of weaker resonances at various positions in the spectrum. Although the methyl groups arising from excess methionine will be metabolized via the one-carbon pool, it is unlikely that other residues would be enriched to a significant degree from the level of methionine used for labeling the enzyme. It was ultimately determined that the use of a restricted second (^{13}C) dimension resulted in the appearance of additional peaks that were aliased into the region containing the methionine methyl resonances. These resonances appear to arise primarily from the natural abundance ^{13}C nuclei of unlabeled lysine or arginine residues. Since a majority of the 32 lysine and 22 arginine residues of rat pol β lie on the surface of the protein, the corresponding resonances tend to exhibit minimal shift dispersion and longer relaxation times characteristic of more flexible side chains. Thus, resonances near 1.78, 1.36, and 1.61 ppm arising from the Hβ, Hγ, and Hδ protons of surface lysine residues, as well as resonances near 1.77 and 1.58 ppm and arising from the Hβ and Hγ protons of surface arginine residues, can be folded into the region of interest. The use of a less restrictive sweep width (24 ppm) eliminated the majority of these aliased resonances; however, there is still a resonance of variable appearance positioned at $\delta(^1H, ^{13}C) = 2.07, 17.04$. This resonance is fairly close to that of free methionine and also was found to exhibit significantly longer T_2 values than those of the remaining methionines (Table 1). For these reasons, we have tentatively assigned this resonance to the amino-terminal methionine, which is incompletely cleaved from the protein (*16*).

To assign the methyl resonances, we prepared a series of mutant enzymes in which each methionine residue was

substituted with a valine residue. Valine was selected since it is one of the commonly occurring mutations for buried methionine residues (*25*). Substitution of valine for methionine residues 18, 236, and 282 yielded pol β mutants in which single peaks in the $^1H-^{13}C$ HSQC spectra were eliminated, making the assignment of the corresponding resonances straightforward. The $^1H-^{13}C$ HSQC spectra for wild-type pol β and M236V and M282V mutants are shown in Figure 2. In contrast with these results, substitution of valine residues for methionine residues 155, 158, and 191 in the C-subdomain resulted in more complex spectral changes. Due to the proximity of these three methionine residues to each other, substitution of any one significantly perturbs the magnetic environment of the remaining two, producing significant chemical shifts. This behavior is illustrated by the effect of the M191V mutation on the $^1H-^{13}C$ HSQC spectrum shown in Figure 3a.

To assign the final three methionine resonances, a variety of alternative strategies were utilized. First, we note that, in the $^1H-^{13}C$ HSQC spectrum of M191V, there is a small shift perturbation of the resonance that we have assigned to Met236 (Figure 3a). Similarly, the methyl resonance of Met191 shows a small shift perturbation in the M236V mutant (Figure 3b). Met191 is located at the beginning of the second strand (residues Met191−Thr196) of sheet 2 of the five-stranded central β-sheet, while Met236 is located on the fourth strand of sheet 2. Thus, while the residues are not spatially close (10.3 Å, Cα to Cα), mutations at residues 191 and 236 appear to transmit small structural perturbations via the β-sheet, explaining the apparent sensitivity of Met236 (Met191) to the M191V (M236V) mutation.

A second strategy involved the use of a ^{13}C-edited NOESY experiment to detect protons in the immediate environment of the methionine methyl resonances (Figure 4). We first note from these spectra that Met1 is unique in exhibiting essentially no NOE cross-peaks, consistent with the assignment of this residue to the amino-terminal methionine, which is largely disordered in all of the reported crystal structures of pol β. Previously reported amino-terminal sequencing of rat pol β that was prepared by a similar procedure has indicated limited microheterogeneity at the amino terminus, so that Met1 is probably partially cleaved in our protein preparation (*16*). To derive assignment information for Met155, Met158, and Met191, we compared the NOESY-HSQC data with the structure of the apo rat pol β (*26*, PDB code 1BPD). Examination of the NOE strips shown in Figure 4 for Met155, Met158, and Met191 indicates large cross-peaks from aliphatic resonances near 1.0 ppm for Met158, and somewhat smaller aliphatic cross-peaks for Met191. Examination of the structure of unliganded rat pol β (*26*) indicates that the Met158 methyl carbon is positioned 4.0 and 4.6 Å from the two methyl groups of Ile150. The Met191 methyl group is 4.0 Å from the Cγ2 methyl of Val162, 4.7 Å from Val193 Cγ2, and at least 5.0 Å from the other methyl groups, while the Met155 methyl group is significantly further from the other methyl groups in its immediate environment. These spatial relationships are consistent with the assignments given in Figure 4, which show the smallest aliphatic cross-peaks for Met155. The NOE strips also indicate weak aromatic cross-peaks for each of these residues. However, relative to the intensity of the diagonal peak, the cross-peak intensity at 7.3 ppm for Met155 is the most intense. From the crystal structure, this methyl group is the closest to any aromatic position, being 3.35 Å from Phe181 Cδ2. The shortest distances to aromatic carbons for both Met158 and Met191 are significantly longer. Many of the shortest internuclear distances correspond to the three methionine residues themselves. For example, the Met191 methyl carbon is 3.8 Å from the Met158 Cβ. Both the

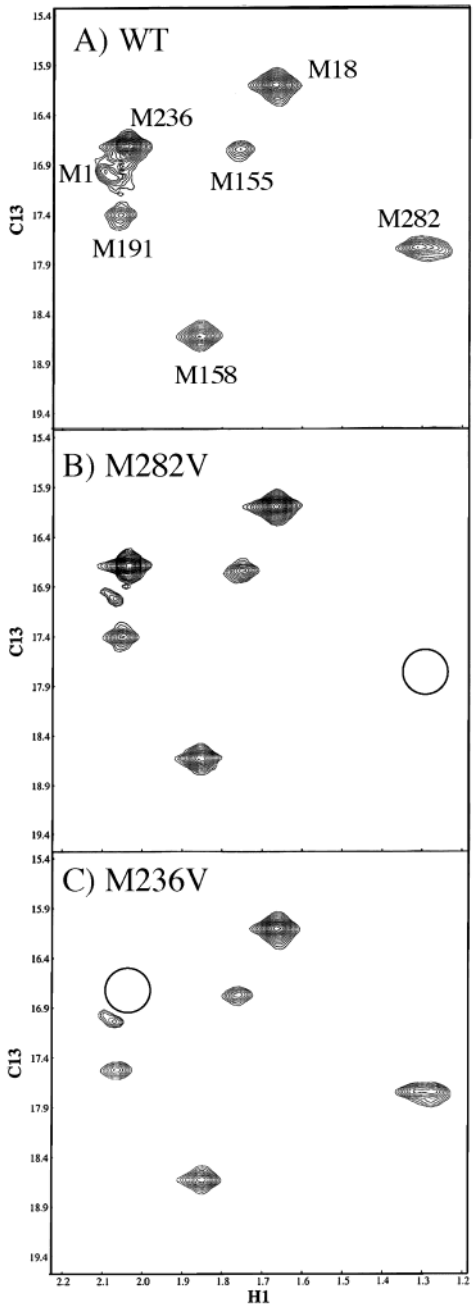

FIGURE 2: $^1H-^{13}C$ HSQC spectra of (A) wild-type [*methyl*-^{13}C]-methionine-labeled rat pol β, (B) M282V [*methyl*-^{13}C]methionine-labeled rat pol β, and (C) M236V rat [*methyl*-^{13}C]methionine-labeled pol β. Sample parameters for (A)−(C): enzyme concentration 0.6, 0.3, and 0.8 mM, respectively. Samples were made in 40 mM Tris-d_{11}, pH 7.6, buffer with 130 mM KCl, 1 mM DTT, 0.1 mM AEBSF, and 0.04% sodium azide in D_2O. The spectra were obtained at 25 °C using Varian's gChsqc pulse sequence on a UNITY INOVA 600 NMR spectrometer with 230 (t_1) × 512 (t_2) complex points and acquisition times of 63.9 ms (t_1) and 64 ms (t_2), corresponding to sweep widths of 24 and 13.3 ppm in the ^{13}C and ^1H dimensions, respectively. Sixteen scans were acquired per increment with a 1.0 s delay between scans.

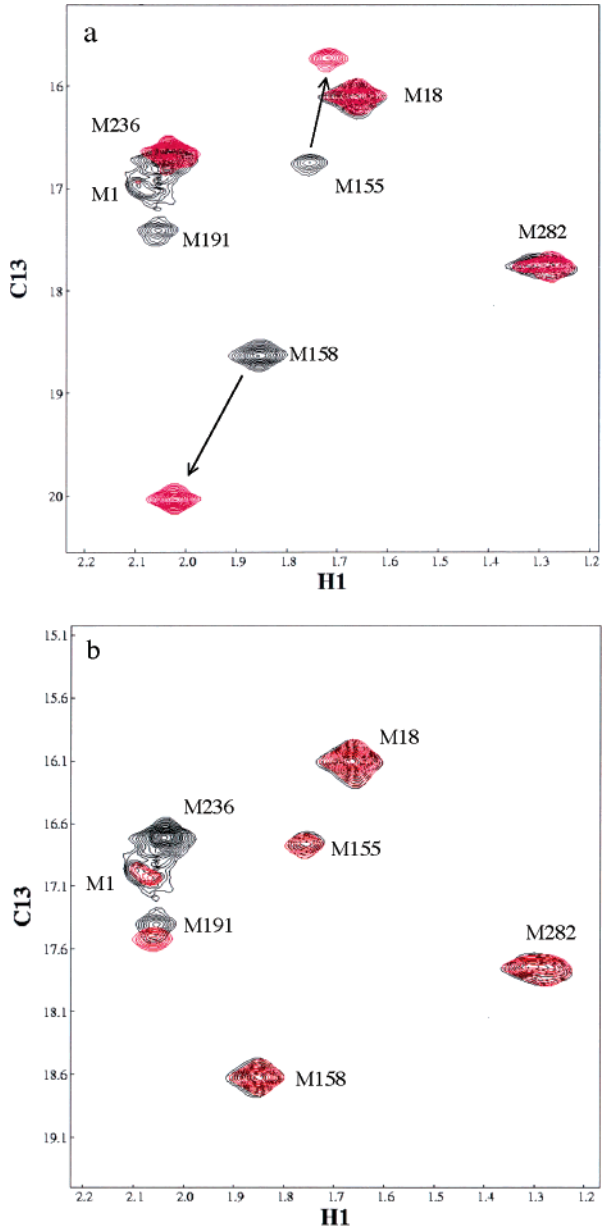

FIGURE 3: (a) Effects of M191V and M236V mutations on the $^{1}H-^{13}C$ HSQC spectra of [*methyl*-^{13}C]methionine-labeled pol β. The spectra for the wild-type enzymes are shown in black, and those for the mutants are shown in red. Substitution of a valine for Met191 results in the disappearance of this resonance and in significant shifts of the methyl resonances of Met155 and Met158, which are located in close proximity to Met191. We note also that Met236 is shifted. (b) Inverse shift perturbation of Met191 resulting from M236V mutation of pol β. In contrast to the close proximity of Met191, Met155, and Met158, the shift perturbations observed for Met191 and Met236 methyl resonances are proposed to be mediated by perturbations of the β-sheet that includes both residues. The enzyme concentration was 0.6 mM (M191V) or 0.8 mM (M236V), in 40 mM Tris-d_{11}, 130 mM KCl, pH 7.6, buffer containing 1 mM DTT, 0.1 mM AEBSF, and 0.04% N_3. NMR spectral parameters were as in Figure 2.

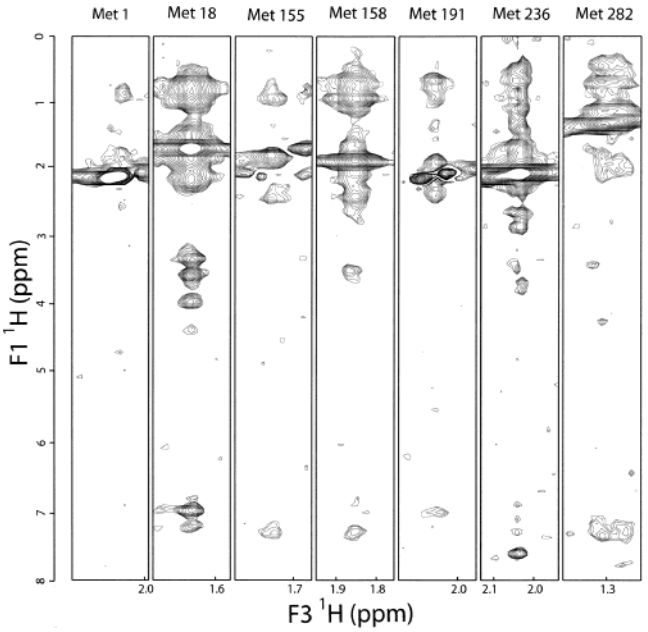

FIGURE 4: ^{13}C-edited NOESY strips for the seven observed methionine resonances. The sample contained 0.6 mM rat [*methyl*-^{13}C]methionine-labeled pol β in the buffer described in Figure 2. The 3D ^{13}C-edited NOESY spectrum was acquired with Varian's gnoesyChsqc experiment (*19*). The spectrum was acquired as a 128 (t_1) $\times$ 36 (t_2) $\times$ 512 (t_3) complex matrix, using a mixing time of 100 ms, with acquisition times of 16.0 ms (t_1), 10.0 ms (t_2), and 64.0 ms (t_3), eight scans per increment, and a 1.0 s recovery delay between scans.

methionine methyl−methyl NOEs and the NOEs to other methionine protons would lead to resonances near 2.0 ppm, which are close to the diagonal and hence difficult to observe. The assignments discussed above are also consistent with the downfield ^{13}C shift for Met158, resulting from its proximity to the edge of the Phe223 phenyl ring. In summary, the NOESY−HSQC data are consistent with the proposed assignments, with the observed aromatic cross-peaks providing the most useful basis for discrimination. However, in the absence of specific assignments for the other proton resonances of the protein, definitive assignment information cannot be obtained.

Two additional features of note in the unliganded pol β HSQC spectra are the variability in the intensity of the Met1 resonance among several different enzyme preparations and the observation of two closely spaced component resonances for residue Met282. In most of the spectra obtained, two Met282 resonances are observed to exhibit similar ^{13}C shifts of 17.66 ppm, and distinct ^{1}H shifts of 1.27 and 1.31 ppm. The structural/conformational basis for the doubled Met282 is not presently clear. However, upon reviewing spectra derived from multiple preparations of the apoenzyme as well as the various mutants, we have found that the intensity of the Met1 peak, which as noted above tends to exhibit significant variability, appears to be correlated with the Met282 1.27/1.31 ppm intensity ratio (Figure 4). Although Met1 and Met282 are located at opposite ends of the pol β sequence, the folded structure observed in the presence of ligands places the lyase domain in close proximity to the N-subdomain (*5*). This suggests that the amino-terminal peptide that is disordered in the crystal may be interacting with residues near Met282. Additional studies will be required to evaluate this possibility more fully.

Paramagnetic Shifts Resulting from Co^{2+} Complexation. The $^{1}H-^{13}C$ HSQC spectra for [*methyl*-^{13}C]pol β were recorded as $MgCl_2$ or $CoCl_2$ was added at millimolar concentration. The former produced negligible shifts, while the latter produced large shifts for Met155 and Met236, and smaller shifts for Met158 and Met191 (Figure 5). Resonances for residues Met18 and Met282, as well as the amino-

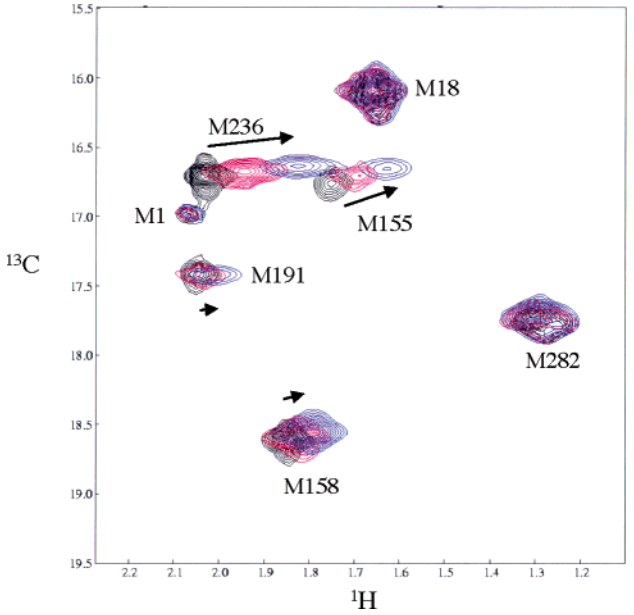

FIGURE 5: ^{1}H−^{13}C HSQC spectra of [*methyl*-^{13}C]methionine-labeled rat pol β as a function of added $CoCl_2$. Samples contained 0.6 mM [*methyl*-^{13}C]methionine-labeled rat pol β in the same buffer described in Figure 2. Samples contained no $CoCl_2$ (black contours), 3 mM $CoCl_2$ (red contours), or 5 mM $CoCl_2$ (blue contours). NMR parameters were as described in Figure 2.

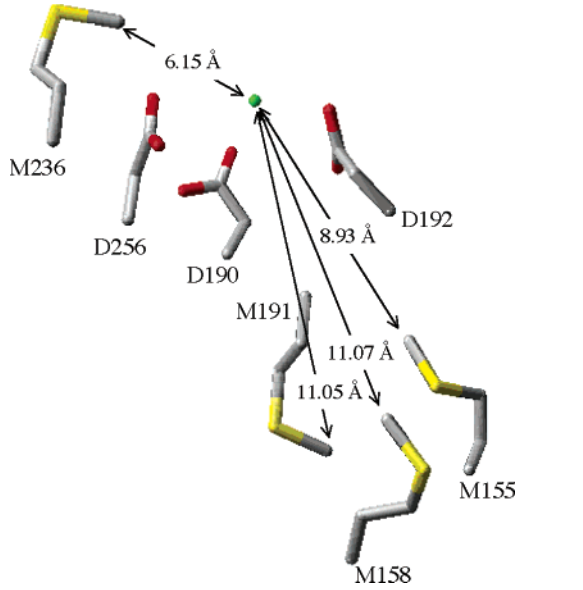

FIGURE 6: Positions of selected residues derived from the structure of a Mn^{2+}−pol β complex (1NOM). The side chains of residues Met155, Met158, Met191, and Met236, as well as the ion binding residues Asp190, Asp192, and Asp156, are shown. The Mn^{2+} ion is shown in green, and the distances between the Mn^{2+} and the methionine methyl carbons are indicated.

terminal methionine resonance, were essentially unaffected. The progressive shifts as a function of Co^{2+} concentration that are apparent in Figure 5 indicate that the exchange of the enzyme between uncomplexed and Co^{2+}-complexed forms is fast to intermediate on the methionine shift time scales, since otherwise separate resonances would be observed for the Co^{2+}-complexed and uncomplexed species. The closest structural model useful for the interpretation of these shifts is a Mn^{2+} complex reported by Pelletier and Sawaya (*27*, PDB code 1NOM). As shown in Figure 6, the metal ion is complexed by aspartyl residues 190, 192, and 256 in the crystal structure. The distances from the Mn^{2+} to the methionine methyl carbons increase for the series Met236 < Met155 < Met191 ≈ Met158, which parallels the magnitude of the observed shifts.

Under fast exchange conditions, the observed shift will be given by

$$\delta_{obs} = p_F\delta_{dia} + p_B\delta_{pc} \quad (1)$$

where p_F and p_B are the fractions of pol β free and complexed with Co^{2+}, δ_{dia} is the shift for the uncomplexed nucleus, and δ_{pc} is the pseudocontact shift resulting from the paramagnetic Co^{2+} ion. The latter is given by (*28*):

$$\delta_{pc} = \frac{\Delta\chi_{ax}}{3Nr_{CoH}^3}(3\cos^2\theta - 1) - \frac{\Delta\chi_{rh}}{2Nr_{CoH}^3}(\sin^2\theta\cos 2\phi) \quad (2)$$

where $\Delta\chi_{ax} = \chi_{zz} - {}^1/_2(\chi_{xx} + \chi_{yy})$, $\Delta\chi_{rh} = \chi_{xx} - \chi_{yy}$, r_{CoH} is the distance between the Co^{2+} ion and the proton (or carbon) under observation, and N is Avogadro's number. If a sufficient number of shifts are observed, the orientation of the **g** tensor can be determined and the shifts of other nuclei can be predicted. In the present case, there is insufficient data for such a determination. However, as is apparent from Figure 6, the angular factors relating the **g** tensor orientation to the methyl nuclei for Met155, Met158, and Met191 are fairly similar, so that the relative shift magnitudes should be inversely related to the distance factors r_{CoH}^{-3} (or r_{CoC}^{-3} for the carbon shifts). Calculations of the maximum possible shift variation using the geometry derived from the crystal structure containing the bound Mn^{2+} ion indicate that even for the most extreme orientation of the **g** tensor the shifts cannot be explained by angular factors alone. The observed shifts are therefore consistent with the assignment of Met155 to the methyl group exhibiting the largest shift among the Met155, Met158, and Met191 resonances. As is apparent from Figure 5, Met236 exhibits an even larger shift, but the angular factor differs significantly for this residue so that a more quantitative analysis is not justified.

Response to dATP. The addition of a complementary nucleotide to a pol β−DNA complex results in both subtle and dramatic conformational changes. In the absence of DNA, it is unclear whether a deoxynucleotide by itself will produce any of these conformational changes. Crystal structures of DNA polymerase−dNTP binary complexes indicate that they are in an open conformation (*26*, *29*, *30*), but the resolution of these structures is insufficient to determine whether subtle local structural changes are induced by dNTP binding to apoenzyme. Addition of a 5.2:1 ratio of Mg^{2+}−dATP to pol β shifted several of the methionine resonances, with Met191 showing the greatest sensitivity (Figure 7). Given the involvement of Asp190 and Asp192 in binding Mg^{2+}−dATP, this result further confirms our resonance assignments. In addition to the shift of Met191, smaller shifts are apparent for Met155 and Met282. In the latter case, the resonance shape becomes more complex, suggesting sampling of multiple conformational states on an intermediate time scale. The shift of the Met282 resonance is, however, significantly smaller than that observed in the presence of gapped DNA plus nucleotide (see below), indicating that the binding of Mg^{2+}−dATP is insufficient to

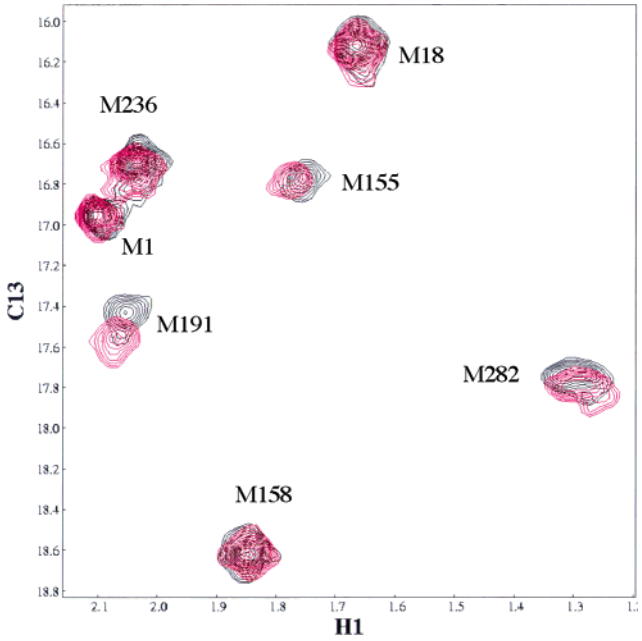

FIGURE 7: Effect of Mg−dATP on the methyl resonances of [*methyl*-^{13}C]methionine-labeled rat pol β. An equimolar mixture of $MgCl_2$ plus dATP was titrated into a sample initially containing 0.6 mM [*methyl*-^{13}C]methionine-labeled pol β (black). The spectrum shown corresponds to a Mg−dATP:pol β ratio of 5.2:1 (in red). The sample was at pH 7.6 in the buffer described in Figure 2.

produce a major conformational change (i.e., subdomain movements resulting in a closed complex). At 12 mM Mg^{2+}−dATP (dATP/enzyme = 23:1), we observe small shifts of Met158 and Met236 as well. Although Met236 may also be sensing a conformational shift, it is possible that, at this high concentration and in the absence of the DNA substrate, there may be nonspecific binding of dATP to the DNA binding site in the vicinity of Met236, which could also serve as the basis for the observed shift.

Relaxation Analysis of Apoenzyme. Table 1 summarizes T_1 and T_2 measurements performed on the methionine residues of the apoenzyme. We note that the significantly longer T_2 value for the resonance assigned to the amino-terminal methionine is consistent with the anticipated motional freedom of this residue. Some systematic variation in the ^{13}C T_1 values is also apparent, with residues Met18, Met236, and Met282 all having values near 2 s, while the three methionine residues in the hydrophobic pocket of the C-subdomain have significantly longer relaxation times in the 2.7−4 s range. Consistent with the discussion of Choy and Kay (*31*), a motional model designated LS-3, which fits effective correlation times, appeared to give the most reasonable results for the order parameters, although the effective correlation times do not provide a physically intuitive basis for understanding the time scales of the dynamic behavior. Inclusion of an R_{ex} term in the fitting of the T_2 data to account for slow exchange motions significantly improved the fit for Met155, for which the resonances clearly show a significant degree of exchange broadening in most of the spectra (e.g., Figures 2 and 3). Smaller R_{ex} values also led to some improvement in fitting the Met191, Met236, and Met282 data as well, while there was no significant improvement for the remaining residues. The order parameters calculated using the LS-3 model are summarized in Table 1, along with order parameter values predicted on the basis of the contact model developed by Ming and Bruschweiler (*32*), and additional details of the analysis are provided as Supporting Information. Values of S^2 range from 0.22 to 0.50, consistent with expectations of low order parameters for the relatively long methionine side chain (*33*). The lower order parameters obtained for Met155, Met158, and Met191 suggest the existence of a more fluid core in the C-subdomain that results from the concentration of aliphatic side chains. However, our calculations fail to verify the anticipated lower order parameter for Met236, on the basis of its location on the protein surface. A significantly lower order parameter for this methyl group is also predicted on the basis of the contact model. The long methionine T_1 values make the relaxation parameters, and particularly the NOE values, difficult to determine accurately due to the failure to utilize sufficiently long interpulse delays, so that alternate labeling approaches such as those described by Kay and co-workers may be preferable for these measurements (*31*, *33*).

Response to Substrates. The response of the methionine methyl resonances to the addition of a series of DNA ligands was also studied. The ligands were added in the following sequence: (1) template strand 16-mer, (2) 5′-phosphorylated downstream 5-mer, and (3) 9-mer upstream primer oligonucleotide. After addition of the three oligonucleotides, a DNA substrate is created with a two-nucleotide gap at the G6−G7 positions of the template, as illustrated in the following diagram:

```
                          98 765 432 1
     Template:   3'-CGA CTA CGC GGC AGC C-5'
                    ||| ||| |||   | ||| |
Upstream Primer: 5'-GCT GAT GCG  pG TCG G-3' :Downstream Oligo
                   123 456 789   1 234 5
```

Addition of a stoichiometric concentration of dideoxycytidine triphosphate (ddCTP) will result in a substrate with a single-nucleotide gap and a dideoxycytidine terminating the primer strand (*5*). Further addition of ddCTP is expected to form an abortive ternary complex with the enzyme, since the primer lacks a 3′-OH required for nucleotide addition.

Upon addition of the template strand, the primary spectral perturbation is a broadening of the Met18 resonance (Figure 8A,B). Met18 does not make contact with the DNA substrate, but is in close proximity with residues on and near the linker connecting the two domains of pol β. Thus, the most probable interpretation of the observed broadening is that the environment of Met18 is affected by the imposition of motional and structural restrictions connecting the polymerase and amino-terminal lyase domains relative to the restrictions characterizing the apoenzyme. It is also possible that there could be exchange broadening due to intermediate exchange kinetics of the ssDNA with the 8 kDa lyase domain. We note, however, that a study of the chemical shifts of the amide resonances of the isolated domain in response to the addition of octyl thymidylate did not identify the Met18 amide resonances as among the more significantly shifted (*35*). The isolated domain lacks the linker helix E that makes up an important component of the local environment of Met18, and thus may not be a good model for this residue in the intact enzyme. An analogous loss of motional independence of the amino-terminal lyase domain upon template binding has also been observed using fluorescence studies of a pol β mutant containing a single tryptophan residue in the lyase domain (F25W) (*34*).

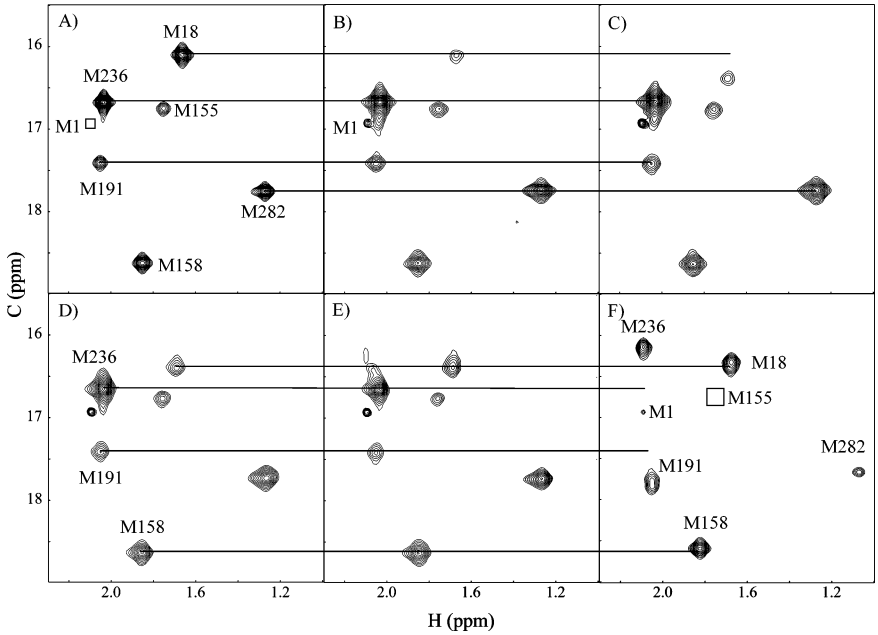

FIGURE 8: Effects of nucleotides on the $^{1}H-^{13}C$ HSQC spectra of [*methyl*-^{13}C]methionine-labeled rat pol β: (A) wild-type rat enzyme; (B) enzyme + DNA template strand; (C) enzyme + DNA template + downstream 5′-phosphate-terminated primer; (D) enzyme + DNA template + downstream primer + primer to form doubly gapped substrate; (E) sample D after the addition of 0.3 mM ddCTP, expected to produce a singly gapped substrate with a primer terminated by dideoxycytidine; (F) sample E + an additional 0.3 mM ddCTP. Horizontal lines in several of the panels facilitate comparisons of the ^{13}C shifts of the corresponding resonances. The enzyme concentration was 0.3 mM, in 5 mM $MgCl_2$, 40 mM Tris-d_{11}, 130 mM KCl, pH 7.6, buffer. Open squares correspond to Met1 in (A) and to Met155 in (F), which were below the threshold of the contour plots.

Subsequent addition of the downstream oligonucleotide produced a pronounced shift of the Met18 resonance and a reduction in the degree of exchange broadening, indicating that the magnetic environment of Met18 has stabilized at a different point than in the apoenzyme. If we consider the apoenzyme as defining state A (Figure 8A) and the enzyme−template−downstream primer complex as defining state B (Figure 8C), then the observed broadening of the Met18 resonance (Figure 8B) in the presence of the template strand could be ascribed to exchange between the A and B states.

To further interpret the series of spectral changes that arise from the addition of nucleotides, it is useful to compare the NMR data with corresponding crystal structures. The most complete structural data available for pol β are for the structures that correspond to the human enzyme in the presence of a gapped DNA substrate (1BPX), a gapped DNA plus a nucleotide (1BPY), and a nicked product DNA complex (1BPZ) formed after the polymerization reaction (*5*). For the apoenzyme, the most similar structure available is 1BPD (*26*) corresponding to the rat enzyme used in the present studies. There are 14 residue differences between the human and rat enzymes, most of which are conservative. The only substitution in the amino-terminal domain is the replacement of Val20 in the rat enzyme with a threonine in the human enzyme, and this residue is not in the immediate vicinity of Met18. Several structural alignments of the lyase domains of 1BPX and 1BPD were performed using various alignment strategies, and all are characterized by significant differences in the conformation of Met18 and the relative position of several nearby residues, particularly Phe76. It is likely that a relative repositioning of Met18 and Phe76 upon addition of template and downstream oligonucleotide strands is the primary cause of the observed Met18 shifts.

Addition of the primer strand to create a DNA substrate with a two-nucleotide gap (Figure 8D) produced minimal spectral changes, even for Met236, which is expected to be in close proximity to the primer 3′-terminus. This may indicate that for the two-nucleotide-gapped substrate, Met236 does not make contact with the primer 3′-terminus. Addition of the first equivalent of ddCTP results in the incorporation of dideoxycytidine to yield a single-nucleotide-gapped DNA structure with a chain-terminating modification at the 3′-primer terminus. This addition resulted in a small perturbation in the shape of the Met236 resonance, suggesting the existence of several different complexes which are in intermediate exchange (Figure 8E). Some broadening of the Met155, Met191, and Met282 methyl resonances was also observed, although these resonances did not shift significantly (compare panels D and E in Figure 8).

Addition of a second equivalent of ddCTP to create an abortive ternary pol β−gapped DNA−nucleotide complex produced dramatic spectral changes (Figure 8F). The Met155 resonance is now broadened below the threshold used in this figure, Met282 and Met191 resonances show significant shifts and broadening, and Met236 is fully shifted to a new position and also shows significant broadening. Met191 is shifted primarily in the ^{13}C dimension, with the peak near $\delta(^{13}C) = 17.75$ ppm, corresponding to $\Delta(^{13}C) = 0.41$ ppm, while Met282 is shifted primarily in the ^{1}H dimension to $\delta(^{1}H) = 1.1$ ppm, or about −0.2 ppm upfield. Resonances for Met1, Met18, and Met158 are not strongly affected by nucleotide addition. The relatively large shifts and broadening for Met155 and Met191 in the C-subdomain, and particularly Met282 in the N-subdomain, are consistent with the conclusion that a major conformational change is occurring in the enzyme upon formation of the abortive complex. We note that none of the corresponding methionine residues are in contact with the substrates, so that the shifts do not result from direct interactions with the bound ligands.

Crystal structure data indicate that nucleotide binding is accompanied by multiple conformational changes. A comparison of the structure of pol β complexed with single-nucleotide-gapped DNA (1BPX) with the structure of gapped DNA plus ddCTP (1BPY) indicates that the primer strand is significantly displaced from its original position relative to Met236. Thus, in going from the pol β−DNA binary complex (1BPX) to the pol β−DNA−ddCTP ternary complex (1BPY), the Met236 methyl group moves away from the deoxyribose of the 3′-terminal nucleotide, and closer to the deoxyribose of the penultimate nucleotide. For example, the distance to the C-5′ of the terminal nucleotide increases from 3.76 to 4.55 Å, while the distance to the C-5′ of the penultimate deoxyriboside decreases from 6.15 to 4.32 Å. These changes in local environment generally are consistent with the shift and broadening observed for Met236 (Figure 8E and F).

DISCUSSION

Enzymatic synthesis of DNA requires a complex set of substrate recognition steps that are accompanied by significant structural changes. The identification of these structures and the dynamic interconversions between them is central to a molecular and thermodynamic description of the basis for efficient and faithful polymerization. In the present study, we have used NMR spectroscopy to study [*methyl*-^{13}C]-methionine-labeled pol β. This labeling approach is completely nonperturbing, and allows structural and dynamic analysis of the enzyme in the vicinity of the six methionine residues (seven including the amino-terminal Met1 residue).

Methionine is a versatile residue that is often located in hydrophobic cores, but can also form part of the interaction surface with substrates or other proteins, and is occasionally involved in hydrogen bonds involving the sulfur as a H-bond acceptor (*36*). For pol β, Met236 is present at the DNA binding site and interacts directly with the primer strand (Figures 1 and 5). In a high-resolution structure (1.65 Å) of a pol β ternary substrate complex (Krahn, Batra, Beard, and Wilson, unpublished data) the sulfur atoms of Met158 and Met282 are within 4 Å of water molecules, and the Met236 sulfur is within 4 Å of the Lys234 Nζ, consistent with the possibility of hydrogen-bonding interactions. Met18 is positioned in a hydrophobic core on the lyase domain and is not observed to be in contact with substrate in any crystallographic structure. However, it does make contact with residues in the linker connecting the two domains of pol β, supporting its utility as an indictor of changes in relative domain orientation and dynamics. Met155, Met158, and Met191 are all involved in a hydrophobic core near the polymerase active site (metal binding ligands Asp190, Asp192, and Asp256). Met282 is of particular interest due to its location near the center of α-helix N, which undergoes a large conformational change upon formation of the ternary complex (*5*).

The Met18 methyl resonance appears to selectively sense the complexation with the templating DNA and the downstream, 5′-phosphorylated oligonucleotide, initially broadening, and subsequently shifting and becoming narrower in the presence of both DNA ligands. Annealing of the downstream oligonucleotide to the template strand results in duplex DNA where the 3′-terminus of the downstream strand is at the blunt end and the 5′-terminus is adjacent to the single-stranded portion of the template strand. Pol β has a high affinity for such 5′-termini when they are phosphorylated even though a 3′-OH is not nearby (*37*, *38*). In contrast with the sensitivity noted above, the Met18 resonance is insensitive to addition of the primer strand, or to formation of the abortive ternary pol β−gapped DNA−ddCTP complex. Although Met18 does not make direct contact with the DNA, its methyl group is positioned near residues Phe76, Leu82, and Leu85 that are in or near the linker connecting the lyase and polymerase domains. The lyase domain plays a critical role in recognition of the 5′-phosphorylated oligonucleotide, and comparison of structures of pol β bound to gapped and nongapped DNA substrates indicates that the lyase and polymerase domains undergo a large reorientation relative to one another (*39*). Thus, the average magnetic microenvironment of the Met18 methyl is shifted in the presence of both the template and 5′-phosphorylated downstream oligonucleotide, while in the presence of template only, there is apparently a slow to intermediate exchange among multiple structures which presumably correspond to variable relative orientations of the two domains.

Conversion of the two-nucleotide-gapped DNA to a single-nucleotide-gapped DNA produces minimal perturbations of the spectrum, with the main variation being the shape of the Met236 resonance. Met236 makes direct contact with the 3′-terminus of the primer strand, so the lack of a significant change suggests that the 3′-terminus may be relatively mobile. A small additional peak is observed for this resonance, which may be due to slowly exchanging conformations of the complex, but could also result from small errors in the nucleotide:pol β concentration ratios. In general, an exact 1:1 DNA−pol β complex is difficult to achieve due to the need to add each nucleotide in the correct proportion. Formation of the ternary pol β−DNA−ddCTP complex resulted in a single, shifted resonance for Met236.

The most significant results of the present study are the large spectral perturbations of the methyl resonances for Met155, Met191, and Met282, shown in Figure 8F, that result from formation of the abortive pol β−gapped DNA−ddCTP complex. These changes indicate a significant conformational change of the enzyme since none of these residues make direct contact with the substrates. Further, although the addition of dATP or gapped DNA produces limited spectral changes, neither interaction alone produces the large perturbations observed upon formation of the abortive ternary complex. These spectral changes are consistent with the conclusion that formation of the ternary complex results in a conformationally activated form of the enzyme. Presumably, this conformational change represents an induced fit of the enzyme to the ternary complex which allows access to, or formation of, the active site so that polymerization can occur.

Crystallographic evidence indicates that, for the abortive pol β−gapped DNA−ddCTP complex that is formed after addition of a second equivalent of ddCTP, there is a significant conformational change, characterized in particular by a rotation of α-helix M that repositions α-helix N (residues 276−287), and by significant conformational changes of residues near the active site, including Asp192, Arg258, Tyr271, Phe272, and Arg283 (*5*). The conformational rearrangement of α-helix N and Arg283 presumably

forms the basis for the observed shift of Met282, while the active site rearrangements, particularly involving Asp192, presumably form the basis for much of the observed chemical shifts of Met155 and Met191. Since dATP alone produces some shifts of these two methionine resonances, these shifts may also indicate some direct contributions of ddCTP binding. The inability of the nucleotide alone to produce the large shifts observed for the ternary complex is consistent with the conclusion that it is only desirable to significantly populate the closed conformation when the nucleotide and the corresponding template base have satisfied a complementarity test by the enzyme. Analogous conclusions have been obtained from fluorescence studies of the L287W/W325A enzyme (*34*), which show that formation of a ternary complex with the correct dNTP dramatically restricts the dynamic behavior monitored by the Trp287 indole ring, while addition of the incorrect dNTP produces minimal dynamic perturbations of Trp287. Thus, the dynamic behavior of the enzyme is influenced by formation of a ternary complex with the correct dNTP.

The behavior of the Met155 resonance in the ternary complex is particularly interesting. While the other methionine resonances exhibit varying degrees of chemical shift as the ternary complex is formed, the Met155 resonance remains severely broadened in the ternary complex. As can be seen from Figure 5, this resonance exhibits the greatest sensitivity to Co^{2+}, and hence is relatively sensitive to the nature of the active site. Crystallographic studies indicate many structural changes near the active site of pol β in going from the complex with gapped DNA to the abortive ternary complex (*5*). For example, the relative distance of the Asp192 carboxyl from the Met155 methyl carbon decreases significantly when the ternary complex is formed. It is possible that the broadening of this resonance represents a conformational cycling of residues near the active site in an attempt to deal with the structural ambiguity presented by the abortive catalytic complex. The broadening of the Met155 and Met191 resonances may also be related to the reversible binding of the second, catalytic Mg^{2+} ion. This binding interaction has been proposed to represent a second, slower step of the conformational transition process (*40*).

The shift of the methyl resonance of Met282 observed upon formation of the ternary complex probably arises from changes in the conformation of the adjacent Arg283 residue, and from the more general rotation of α-helix N on which Met282 is located (*5*). Arg283 interacts with the templating base and sugar of the following (i.e., 3′) templating nucleotide when α-helix N has moved to the "closed" position upon formation of the ternary complex. It has been suggested that the rate-limiting step in the polymerase reaction may involve repositioning of critical side chains including Asp192, Arg258, Phe272, Arg283, and Glu295 (*9*, *34*, *41*). The observed exchange broadening of the Met282 methyl resonance in the ternary complex could reflect some of these conformational changes, particularly involving the adjacent Arg283 residue. Recently, an enzyme with a leucine substitution at this position (M282L) has been characterized (*42*). This mutant exhibited diminished fidelity and increased stability, suggesting that dynamic perturbations have an important role in nucleotide discrimination. These observations are consistent with a critical interaction between Met282 and Arg283 in the polymerization process. Alanine substitution for Arg283 (R283A) dramatically decreases catalytic efficiency of correct nucleotide insertion (*6*, *11*), base substitution fidelity (*6*, *43*), and frameshift fidelity (*44*). Accordingly, Met282 substitutions may indirectly influence fidelity through perturbation of the adjacent arginine residue.

Table 2: Methionine Methyl *B* Factors from Published Crystal Structures[a]

	1BPD	1BPX	1BPY
ligands	none	gapped DNA	gapped DNA + ddCTP
resolution (Å)	3.60	2.40	2.20
Met residue			
Met18	69.59	45.88	63.17
Met155	44.69	50.85	75.47
Met158	28.56	50.44	51.34
Met191	27.52	65.03	37.73
Met236	68.41	53.66	56.00
Met282	68.56	52.21	61.90

[a] The entries correspond to published crystal structures (1BPD (*26*); 1BPX and 1BPY (*5*)). 1BPD corresponds to the apoenzyme from rat; 1BPX and 1BPY correspond to the human enzyme complexed with a gapped DNA substrate and an abortive ternary complex, respectively.

A comparison of the relaxation and resonance broadening data with crystallographic *B* factors for the methionine methyl carbons (Table 2) revealed several weak correlations. In the structure of the apoenzyme (*26*, PDB code 1BPD), the three methionine residues in the C-subdomain that exhibit longer T_1 values (Met155, Met158, and Met191) also exhibit lower *B* factors (Table 2). This result would be consistent with a reduced degree of segmental motion, which probably contributes significantly to the R_1 relaxation rate. Diffusion about the methyl axis would not be expected to contribute to the crystallographic *B* factor. In contrast, Met18, Met236, and Met282 have significantly higher *B* factors. A comparison of the *B* factors observed in 1BPX, corresponding to the pol β−single-nucleotide-gapped DNA complex, with the *B* factors for 1BPY, corresponding to the pol β−gapped DNA−ddCTP ternary complex, shows a 50% increase for Met155. This observation is consistent with the significant degree of exchange broadening observed for this resonance upon formation of the ternary complex (Figure 8F). The *B* factor for Met282 is also increased. However, the changes observed for Met18, Met191, and Met236 do not follow the pattern suggested by the observed exchange broadening. Since the effects of static disorder and dynamic processes are both included in the observed *B* factors, the correlation with NMR relaxation data is typically limited.

The data presented here demonstrate that methionine labeling represents a particularly useful approach for studying the conformational and dynamic behavior of pol β in solution. The distribution of methionine residues facilitates the evaluation of how ligands influence global (domain/subdomain) and local dynamics. The results extend crystallographic structural information and provide insight into the dynamic properties of the enzyme during ligand binding. Specifically, the observed broadening of resonances for Met155, Met191, and Met282 that is observed in the abortive pol β−gapped DNA−ddCTP ternary complex indicates a more dynamic state than is observed for the apoenzyme or implied from crystallographic snapshots of liganded forms of pol β. This approach will provide a useful means for evaluating the dynamic behavior of site-directed mutant enzymes. Coupled with kinetic and/or thermodynamic char-

acterization, such studies will provide insight into the relationship of conformational dynamics and polymerase fidelity.

ACKNOWLEDGMENT

We are grateful to Dr. Joseph Krahn for providing the coordinates on an unpublished, high-resolution structure of a pol β complex. We are also grateful to Prof. Rafael Bruschweiler and Dr. Dengming Ming, Clark University, for providing the calculated order parameters for pol β based on their contact model.

SUPPORTING INFORMATION AVAILABLE

Additional details of the analysis of the NMR relaxation data. This material is available free of charge via the Internet at http://pubs.acs.org.

REFERENCES

1. Beard, W. A., and Wilson, S. H. (2000) Structural design of a eukaryotic DNA repair polymerase: DNA polymerase beta, *Mutat. Res.—DNA Repair 460*, 231−244.
2. Wood, R. D., Mitchell, M., Sgouros, J., and Lindahl, T. (2001) Human DNA Repair Genes, *Science 291*, 1284−1289.
3. Ollis, D. L., Brick, P., Hamlin, R., Xuong, N. G., and Steitz, T. A. (1985) Structure of large fragment of Escherichia coli DNA polymerase 1 complexed with dTMP, *Nature 313*, 762−766.
4. Pelletier, H., Sawaya, M. R., Kumar, A., Wilson, S. H., and Kraut, J. (1994) Structures of ternary complexes of rat DNA-polymerase β, a DNA template-primer, and ddCTP, *Science 264*, 1891−1903.
5. Sawaya, M. R., Prasad, R., Wilson, S. H., Kraut, J., Pelletier, H. (1997) Crystal structures of human DNA polymerase beta complexed with gapped and nicked DNA: evidence for an induced fit mechanism, *Biochemistry 36*, 11205−11215.
6. Beard, W. A., Osheroff, W. P., Prasad, R., Sawaya, M. R., Jaju, M., Wood, T. G., Kraut, J., Kunkel, T. A., and Wilson, S. H. (1996). Enzyme-DNA interactions required for efficient nucleotide incorporation and discrimination in human DNA polymerase β, *J. Biol. Chem. 271*, 12141−12144.
7. Ahn, J., Werneburg, B. G., and Tsai, M. D. (1997). DNA polymerase β: Structure-fidelity relationship from pre-steady-state kinetic analyses of all possible correct and incorrect base pairs for wild type and R283A mutant, *Biochemistry 36*, 1100−1107.
8. Kraynov, V. S., Werneburg, B. G., Zhong, X. J., Lee, H., Ahn, J. W., and Tsai, M. D. (1997) DNA polymerase beta: Analysis of the contributions of tyrosine-271 and asparagine-279 to substrate specificity and fidelity of DNA replication by pre-steady-state kinetics, *Biochem. J. 323*, 103−111; Erratum *325*, 815.
9. Vande Berg, B. J., Beard, W. A., and Wilson, S. H. (2001) DNA structure and aspartate 276 influence nucleotide binding to human DNA polymerase β: Implication for the identity of the rate-limiting conformational change, *J. Biol. Chem. 276*, 3408−3416.
10. Beard, W. A., Shock, D. D., Yang, X.-P., DeLauder, S. F., and Wilson, S. H. (2002) Loss of DNA polymerase β stacking interactions with templating purines, but not pyrimidines, alters catalytic efficiency and fidelity, *J. Biol. Chem. 277*, 8235−8242.
11. Beard, W. A., Shock, D. D., Vande Berg, B. J., and Wilson, S. H. (2002). Efficiency of correct nucleotide insertion governs DNA polymerase fidelity, *J. Biol. Chem. 277*, 47393−47398.
12. Blakley, R. L., Cocco, L., London, R. E., Walker, T. E., and Matwiyoff, N. A. (1978) Nuclear magnetic resonance studies on bacterial dihydrofolate reductase containing [methyl-^{13}C] methionine, *Biochemistry 17*, 2284−2293.
13. London, R. E., and Avitabile, J. (1978) Calculated ^{13}C NMR relaxation parameters for a restricted internal diffusion model. Application to methionine relaxation in dihydrofolate reductase, *J. Am. Chem. Soc. 100*, 7159−7165.
14. Beatty, E. J., Cox, M. C., Frenkiel, T. A., Tam, B. M., Mason, A. B., MacGillivray, R. T. A., Sadler, P. J., and Woodworth, R. C. (1996) Interlobe communication in ^{13}C methionine-labeled human transferrin, *Biochemistry 35*, 7635−7642.
15. Kleerekoper, Q., and Putkey, J. A. (1999) Drug binding to cardiac Troponin C, *J. Biol. Chem. 274*, 23932−23939.
16. Kumar, A., Widen, S. G., Williams, K. R., Kedar, P., Karpel, R. L., and Wilson, S. H. (1990) Studies of the domain structure of mammalian DNA polymerase β, *J. Biol. Chem. 265*, 2124−2131.
17. Muchmore, D. C., McIntosh, L. P., Russell, C. B., Anderson, D. E., and Dahlquist, F. W. (1989) Expression and N-15 labeling of proteins for proton and N-15 nuclear magnetic resonance, *Methods Enzymol. 177*, 44−73.
18. John, B. K., Plant, D., and Hurd, R. E. (1993) Improved proton-detected heteronuclear correlation using gradient-enhanced Z and ZZ filters, *J. Magn. Reson., A 101*, 113−117.
19. Muhandiram, D. R., Farrow, N. A., Xu, G.-Y., Smallcombe, S. H., and Kay, L. E. (1993) A gradient ^{13}C NOESY-HSQC experiment for recording NOESY spectra of ^{13}C-labeled proteins dissolved in H_2O, *J. Magn. Reson. B 102*, 317−321.
20. Delaglio, F., Grzesiek, S., Vuister, G. W., Zhu, G., Pfeifer, J., and Bax, A. (1995) NMRPipe: A multidimensional spectral processing system based on UNIX pipes. *J. Biomol. NMR 6*, 277−293.
21. Johnson, B. A., and Blevins, R. A. (1994) NMRVIEW: a computer program for the visualization and analysis of NMR data, *J. Biomol. NMR 4*, 603−614.
22. Zhu, G., and Bax, A. (1992) Improved linear prediction of damped NMR signals using modified forward−backward linear prediction, *J. Magn. Reson. 100*, 202−207.
23. Farrow, N. A., Muhandiram, R., Singer, A. U., Pascal, S. M., Kay, C. M., Gish, G., Shoelson, S. E., Pawson, T., Forman-Kay, J. D., and Kay, L. E. (1994). Backbone dynamics of a free and phosphopeptide-complexed Src homology 2 domain studied by ^{15}N NMR relaxation, *Biochemistry 33*, 5984−6003.
24. Yamazaki, T., Muhandiram, R., and Kay, L. E. (1994). NMR Experiments for the Measurement of Carbon Relaxation Properties in Highly Enriched, Uniformly ^{13}C,^{15}N-Labeled Proteins—Application to $^{13}C^{\alpha}$ Carbons, *J. Am. Chem. Soc. 116*, 8266−8278.
25. Bordo, D., and Argos, P. (1991) Suggestions for "safe" residue substitutions in site-directed mutagenesis, *J. Mol. Biol. 217*, 721−729.
26. Sawaya, M. R., Pelletier, H., Kumar, A., Wilson, S. H., and Kraut, J. (1994) Crystal structure of rat DNA polymerase β: Evidence for a common polymerase mechanism, *Science 264*, 1930−1935.
27. Pelletier, H., and Sawaya, M. R. (1996) Characterization of the metal ion binding helix-hairpin-helix motifs in human DNA polymerase beta by X-ray structural analysis, *Biochemistry 35*, 12778−12787.
28. Emerson, S. D., and La Mar, G. N. (1990) NMR determination of the orientation of the magnetic-susceptibility tensor in cyanometmyoglobin—a new probe of steric tilt of bound ligand, *Biochemistry 29*, 1556−1566.
29. Beese, L. S., Friedman, J. M., and Steitz, T. A. (1993) Crystal structures of the Klenow fragment of DNA polymerase I complexed with deoxynucleoside triphosphate and pyrophosphate, *Biochemistry* 32, 14095−14101.
30. Li, Y., Kong, Y., Korolev, S., and Waksman, G. (1998). Crystal structures of the Klenow fragment of *Thermus aquaticus* DNA polymerase I complexed with deoxyribonucleoside triphosphates, *Protein Sci. 7*, 1116−1123.
31. Choy, W.-Y., and Kay, L. E. (2003) Model selection for the interpretation of protein side chain methyl dynamics, *J. Biomol. NMR 25*, 325−333.
32. Ming, D., and Bruschweiler, R. (2004) Prediction of methyl-side chain dynamics in proteins, *J. Biomol. NMR* (in press).
33. Skrynnikov, N. R., Millet, O., and Kay, L. E. (2002) Deuterium spin probes of side-chain dynamics in proteins. 2. Spectral density mapping and identification of nanosecond time-scale side-chain motions, *J. Am. Chem. Soc. 124*, 6449−6460.
34. Kim, S.-J., Beard, W. A., Harvey, J., Shock, D. D., Knutson, J. R., and Wilson, S. H. (2003) Rapid segmental and subdomain motions of DNA polymerase β, *J. Biol. Chem. 278*, 5072−5081.
35. Liu, D., Prasad, R., Wilson, S. H., DeRose, E. F., and Mullen, G. P. (1996) Three-dimensional solution structure of the N-terminal domain of DNA polymerase β and mapping of the ssDNA interaction interface, *Biochemistry 35*, 6188−6200.
36. Gregoret, L. M., Rader, S. D., Fletterick, R. J., and Cohen, F. E. (1991) Hydrogen-bonds involving sulfur atoms in proteins, *Proteins: Struct., Funct., Genet. 9*, 99−107.

37. Prasad, R., Beard, W. A., and Wilson, S. H. (1994) Studies of gapped DNA substrate-binding by mammalian DNA polymerase β. Dependence on 5′-phosphate group, *J. Biol. Chem. 269*, 18096−18101.
38. Husain, I., Morton, B. S., Beard, W. A., Singhal, R. K., Prasad, R., Wilson, S. H., and Besterman, J. M. (1995) Specific inhibition of DNA polymerase β by its 14 kDA domain—role of single-stranded and double-stranded DNA binding and 5′-phosphate recognition, *Nucleic Acids Res. 23*, 1597−1603.
39. Beard, W. A., and Wilson, S. H. (1998) Structural insights into DNA polymerase β fidelity: hold tight if you want it right, *Chem. Biol. 5*, R7−R13.
40. Arndt, J. W., Gong, W., Zhong, X., Showalter, A. K., Liu, J., Dunlap, C. A. Lin, Z., Paxson, C., Tsai, M.-D., and Chan, M. K. (2001) Insight into the catalytic mechanism of DNA polymerase β: structures of intermediate complexes, *Biochemistry 40*, 5368−5375.
41. Yang, L. J., Beard, W. A., Wilson, S. H., Roux, B., Broyde, S., and Schlick, T. (2002) Local deformations revealed by dynamics simulations of DNA polymerase β with DNA mismatches at the primer terminus, *J. Mol. Biol. 321*, 459−478.
42. Shah, A. M., Conn, D. A., Li, S.-X., Capaldi, A., Jager, J., and Sweasy, J. B. (2001) A DNA polymerase β mutator mutant with reduced nucleotide discrimination and increased protein stability, *Biochemistry 40*, 11372−11381.
43. Osheroff, W. P., Jung, H. K., Beard, W. A., Wilson, S. H., and Kunkel, T. A. (1999) The fidelity of DNA polymerase beta during distributive and processive DNA synthesis, *J. Biol. Chem. 274*, 3642−3650.
44. Osheroff, W. P., Beard, W. A., Yin, S., Wilson, S. H., and Kunkel, T. A. (2000) Minor groove interactions at the DNA polymerase beta active site modulate single-base deletion error rates, *J. Biol. Chem. 275*, 28033−28038.
45. Koradi, R., Billeter, M., and Wuthrich, K. (1996) MOLMOL—a program for display and analysis of macromolecular structures, *J. Mol. Graphics 14*, 51−55.

BI049641N